

Targeted Ablation of Connexin50 in Mice Results in Microphthalmia and Zonular Pulverulent Cataracts

Thomas W. White, Daniel A. Goodenough, and David L. Paul

Department of Cell Biology and Department of Neurobiology, Harvard Medical School, Boston, Massachusetts 02115

Abstract. In the ocular lens, gap junctional communication is a key component of homeostatic mechanisms preventing cataract formation. Gap junctions in rodent lens fibers contain two known intercellular channel-forming proteins, connexin50 (Cx50) and Cx46. Since targeted ablation of Cx46 has been shown to cause senile-type nuclear opacities, it appears that Cx50 alone cannot meet homeostatic requirements. To determine if lens pathology arises from a reduction in levels of communication or the loss of a connexin-specific function, we have generated mice with a targeted deletion of the Cx50 gene. Cx50-null mice exhibited microphthalmia and nuclear cataracts. At postnatal day 14 (P14), Cx50-knockout eyes weighed 32% less than controls, whereas lens mass was reduced by 46%. Cx50-

knockout lenses also developed zonular pulverulent cataracts, and lens abnormalities were detected by P7. Deletion of Cx50 did not alter the amounts or distributions of Cx46 or Cx43, a component of lens epithelial junctions. In addition, intercellular passage of tracers revealed the persistence of communication between all cell types in the Cx50-knockout lens. These results demonstrate that Cx50 is required not only for maintenance of lens transparency but also for normal eye growth. Furthermore, these data indicate that unique functional properties of both Cx46 and Cx50 are required for proper lens development.

Key words: lens • gap junction • connexin • microphthalmia • cataract

IN the vertebrate lens, every cell is directly coupled to its neighbors by the intercellular channels that comprise gap junctions. These channels join the cells of the crystallin lens into a functional syncytium, allowing adjacent cells to directly share ions, second messengers, and metabolites. Since the lens is an avascular cyst, gap junctions allow cells in the interior of the organ to gain access to metabolites absorbed at the surface from the aqueous humor (Goodenough et al., 1980), providing a critical mechanism for metabolite exchange.

The lens has two distinct types of cells; a simple cuboidal epithelium lines the anterior surface and differentiated fibers constitute the rest of the lenticular mass. Mitotically active epithelial cells at the lens equator differentiate to give rise to the lens fibers, which lose intracellular organelles and accumulate high concentrations of soluble proteins known as crystallins (Piatigorsky, 1981). These cellular properties, together with an elastic capsule and zonular fibers, result in the optical transparency, high refractive index, and elasticity necessary for accommodation. With the loss of cellular organelles, the fibers lose the

ability to support oxidative phosphorylation and an active metabolism. It has been proposed that intercellular communication allows the metabolically active epithelium to maintain the precise intracellular ionic conditions necessary to prevent precipitation of the crystallins and cataract formation (Goodenough, 1979; Rae, 1979; Mathias et al., 1997).

The structural proteins comprising intercellular channels, the connexins (Cx)¹, are a multigene family consisting of at least 14 members, three of which are expressed in the lens (Bruzzone et al., 1996; Kumar and Gilula, 1996). Junctions between rodent lens epithelial cells contain predominantly Cx43 (Beyer et al., 1989). During differentiation into fibers, Cx43 expression is downregulated and replaced by two different connexins, Cx46 and Cx50 (Kistler et al., 1985; Paul et al., 1991; White et al., 1992). Each connexin forms channels with distinctly different physiological properties of gating, permeation, and selective interaction with other connexins. It has been shown that in the *Xenopus* oocyte pair assay, cells expressing Cx43 can form intercellular channels with cells expressing Cx46 but not

Address correspondence to David L. Paul, Department of Neurobiology, Harvard Medical School, Boston, MA 02115. Tel.: (617) 432-1203. Fax: (617) 432-2955. E-mail: dpaul@hms.harvard.edu

1. *Abbreviations used in this paper:* Cx, connexin; Cx50, connexin50; E, embryonic day; P, postnatal day.

Cx50 (White et al., 1994), raising the possibility that communication may not be equivalent in all regions of the lens.

The hypothesis that intercellular communication is critical for lens development and homeostasis can be tested by targeted ablation of lens connexin genes. Cx46-knockout mice display a progressive "senile-type" cataractogenesis, with otherwise normal ocular development (Gong et al., 1997). This observation supports the idea that junctional communication influences homeostatic mechanisms in the lens. The ability of fibers to communicate in these animals, although not directly analyzed, is likely to persist because Cx50 distribution is unaffected. Thus, cataracts in the Cx46-knockout could develop either from a simple reduction in the absolute number of intercellular channels, regardless of connexin type, or because the presence of Cx46 provides an activity not obtainable from Cx50 alone. The first possibility would be supported if targeted disruption of the Cx50 and Cx46 genes produced the same phenotype, whereas the second possibility predicts that different phenotypes would result.

To explore this question, we have produced a targeted ablation of the murine Cx50 gene that resulted in a unique phenotype from that seen in the Cx46-knockout animals. Cataracts developed in the Cx50-knockout animals with a different time course and with a distinctly different cataractogenic process characterized by zonular pulverulent nuclear opacities. In addition, the Cx50-knockout mice showed a defect in the growth of both the lens and the eye, a phenotype not observed in the Cx46-knockout animals. Taken together, these data demonstrate that intercellular communication is essential for multiple aspects of lens development and function, and that Cx46 and Cx50 each play unique roles. In addition, the Cx50-knockout mice provide a model for congenital cataracts caused by mutations recently identified in the human Cx50 gene (Shiels et al., 1998).

Materials and Methods

Generation of Cx50-deficient Mice

A Cx50 genomic clone was isolated from a 129/Sv mouse genomic library (gift of E. Li, Massachusetts General Hospital, Boston, MA) using a coding region probe (White et al., 1992). A replacement targeting vector containing a pgk-neo cassette was designed to delete the entire coding region (see Fig. 1). The vector contained 5' and 3' homology regions of 1.3 and 7.1 kb, respectively, inserted into the pPNT vector and included a pgk-TK cassette downstream of the 5' homology region. The vector was electroporated into J1 ES cells (gift of E. Li) and near-FIAUr clones were isolated by positive/negative selection as described (Li et al., 1992). Homologous recombinants were identified by PCR screening using a 5' flanking primer (pcr 1; 5'-GCCCCCTCCTGCTTATTCTG) and a 3' primer derived from vector sequences unique to the replacement cassette (pcr 2; 5'-CGGGCCTCTTCGCTATTACG) and were obtained at a frequency of 1 in 60 near-FIAUr colonies. Two independent disrupted Cx50 ES cell clones were injected into C57BL/6J blastocysts to produce chimeric animals (Li et al., 1992). Male chimeras were bred with C57BL/6J females to generate F1 hybrid mice. Matings of F1 heterozygotes produced all three expected genotypes in a Mendelian ratio. Male founders exhibiting high rates of germline transmission were bred with 129/Sv females to obtain the mutated Cx50 allele in a pure 129/Sv genetic background.

For genotyping animals, pcr 1 was paired with either pcr 2 or a third primer derived from the Cx50-coding region (pcr 3; 5'-CTCCATGC-GAACGTGGTG TAC). Primers 1 + 2 amplified a 1370-bp band from knockout chromosomes. Amplification of wild-type chromosomes with

primers 1 + 3 produced a 1,600-bp band. Genomic structure was also confirmed by Southern blotting. NcoI-digested ES cell or tail DNA was probed with a fragment from the 5' homology region common to wild-type and targeted chromosomes. A 5.5-kb band was expected for wild-type alleles, and a 3.8-kb band was diagnostic of knockout alleles.

Light Microscopy

Embryonic (E16) and adult mouse lenses were fixed in 1% formaldehyde, freshly prepared from paraformaldehyde, in phosphate buffered saline (PBS) for 1 h at room temperature. Fixed lenses were rinsed in PBS, embedded in OCT (Miles, Elkhart, IN), and then frozen in liquid nitrogen. 10- μ m frozen sections were prepared and processed as previously described (Paul et al., 1991). Sections were incubated with anti-Cx50 antiserum (White et al., 1992) diluted 1:100, anti-Cx46 antiserum (Paul et al., 1991) diluted 1:100, or affinity-purified anti-Cx43 antibody (Goliger and Paul, 1994) diluted 1:200 with 1% normal goat serum and 2% BSA in PBS, for 1 h at room temperature. Sections were washed in PBS and then incubated with rhodamine-conjugated goat anti-rabbit antiserum. For histological analysis, embryonic eyes or neonatal lenses were fixed in 4% formaldehyde in PBS for 16–24 h. After rinsing in PBS, samples were dehydrated and embedded in paraffin. Sections of 1 μ m were cut on a diamond knife, deparaffinized, and then stained with hematoxylin and eosin.

Electron Microscopy

Lenses from 10-d-old animals were fixed in 2.5% glutaraldehyde and 1% tannic acid in 0.1 M sodium cacodylate buffer, pH 7.4 (cacodylate), for 4 h at room temperature. After washing in cacodylate, specimens were then cut into quadrants, postfixed in 1% OsO₄ in cacodylate, and then washed in distilled water. The lenses were stained en bloc with 1% uranyl acetate in water, washed in water, and dehydrated in ethanols and propylene oxide, and then embedded in Epon 812, oriented to permit cross sections through the lens equator. Cross sections from equivalent equatorial lens regions were photographed at 4,000 \times electron optical magnification and three times photographic prints used to measure cell diameters. 163 cell diameters in nine separate fields were measured across the short axes of the lens fibers to obtain the data set presented in the Results.

Gel Electrophoresis and Western Blotting

For crystallin analysis, lenses were dissected from 6-mo-old Cx50 (+/+) and (-/-) mice. Equal wet weights of wild-type and knockout lens were homogenized in 10 ml of 0.1 M NaCl, 0.1 M Na₂HPO₄, pH 7.4, containing 10 mM ascorbic acid (as an antioxidant) and centrifuged at 14,000 g for 20 min at 20°C and the supernatants containing soluble lens proteins were collected. The insoluble pellets were then sequentially washed with 10 ml of 0.1 M NaCl, 0.1 M Na₂HPO₄, pH 7.4, extracted with 10 ml of 20 mM NaOH, and washed with 10 ml of 1 mM Na₂CO₃. The final insoluble pellet was resuspended in 1 ml of 1 \times SDS sample buffer containing 10 mM DTT. Protein concentrations of each extraction step were determined using the bicinchoninic acid assay (Pierce Chemical Co., Rockford, IL). Equal volumes of lens fractions from each extraction step were electrophoresed on 15% polyacrylamide gels and transferred to nitrocellulose membranes, or silver stained (Blum et al., 1987). Western blots were probed with antibodies to α A-, α B-, or γ -crystallin (provided by J. Horowitz, Jules Stein Eye Institute, University of California, Los Angeles, CA).

For connexin analysis, adult lenses were collected and equal wet weights were homogenized on ice in 5 mM Tris-HCl, pH 8.0, 1 mM EDTA, 1 mM EGTA, containing 20 μ M PMSF and 10 μ g/ml leupeptin (lysis buffer). The homogenate was centrifuged at 100,000 g at 4°C for 30 min, the membrane pellet resuspended in fresh lysis buffer, and the protein concentration determined using the BCA assay (Pierce Chemical Co., Rockford, IL). Equal protein concentrations from wild-type and knockout lenses were electrophoresed, transferred, and probed with the same antiserum used for light microscopy. Primary antibodies were detected with alkaline phosphatase-conjugated goat anti-rabbit IgG (Boehringer Mannheim, Indianapolis, IN) using nitro blue tetrazolium and 5-bromo-4-chloro-3-indolyl phosphate as substrates (Sigma Chemical Co., St. Louis, MO).

Dye Injection

Embryonic lenses (E15.5) were dissected at 37°C from the enucleated globe in M199 culture medium buffered with 10 mM Hepes, pH 7.4 (M199). After a brief incubation in 1% collagenase and 1% hyaluronidase

in M199, the tunica vascularis could be grasped with fine forceps and removed. Lenses were then mounted on their equatorial edges in 35-mm polylysine-coated dishes in M199 culture medium. High resistance microelectrodes were filled at the tip with a solution of 2% Lucifer yellow (Molecular Probes, Eugene, OR) and 2% neurobiotin (Vector Laboratories, Burlingame, CA) by capillary action. Electrodes were then backfilled with 100 mM LiCl₂. Centrally located epithelial cells were impaled from the anterior lens surface, and fibers were impaled from either anterior (through the epithelium) or posterior surfaces. Dyes were ionophoretically injected for 10 min using 5-nA current pulses of 500 ms duration at a frequency of 1 Hz. Injected lenses were photographed, fixed in 4% formaldehyde freshly made from paraformaldehyde, and then processed for paraffin embedding. Lenses were serially sectioned, deparaffinized, and rehydrated. Sections were incubated with rhodamine-conjugated avidin (Pierce Chemical Co.) and diluted 1:500 with PBS containing 1% normal goat serum and 2% BSA for 1 h at room temperature. Sections were washed in PBS and photographed with epifluorescence.

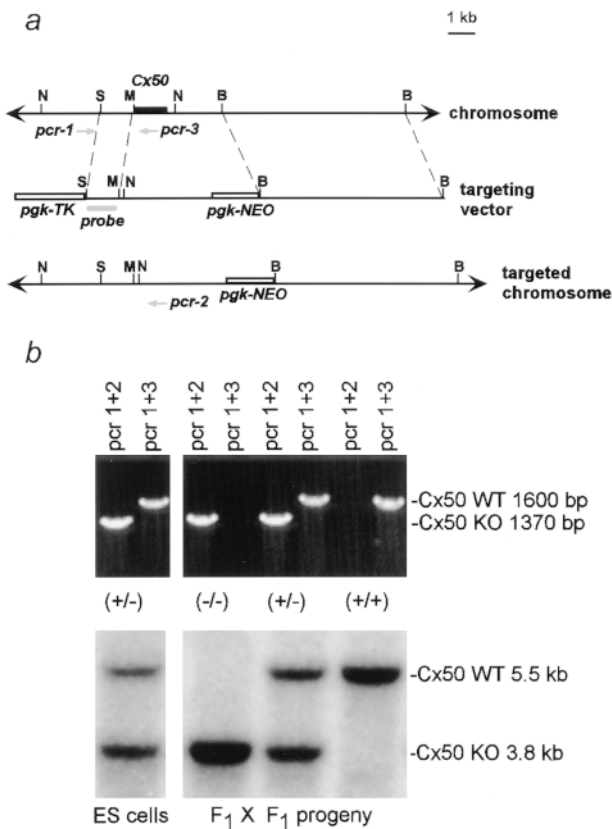


Figure 1. Targeting strategy for inactivation of the Cx50 gene and genotyping of generated mice. (a) The genomic structure near Cx50, whose coding region is contained within a single exon. A replacement targeting vector containing a pgk-neo cassette was flanked by 5' and 3' homology regions of 1.3 and 7.1 kb, respectively, and included a pgk-TK cassette downstream of the 5' homology region. (b) For genotyping, a 5' flanking primer (*pcr 1*) was paired with either a 3' primer derived from specific sequences in the replacement cassette (*pcr 2*) or a primer derived from the Cx50 coding region (*pcr 3*). Primers 1 + 2 amplified a 1,370-bp band from knockout chromosomes. Amplification of wild-type chromosomes with primers 1 + 3 produced a 1,600-bp band. Genomic structure was confirmed by probing Southern blots of Nco1-digested ES cell or tail DNA with a fragment from the 5' homology region common to both alleles. A 5.5-kb band was expected for wild-type alleles, and a 3.8-kb band was diagnostic of knockout alleles. Only relevant restriction enzyme sites are shown: N, Nco1; S, SacI; M, MscI; B, BamHI.

Results

Targeted Disruption of the Connexin50 Gene

Embryonic stem cells heterozygous for the Cx50 gene were generated by homologous recombination. Maps of the wild-type Cx50 locus, the Cx50 targeting vector, and the disrupted Cx50 locus are shown in Fig. 1 a. Like many other connexin genes, the coding sequence of Cx50 is contained within a single exon (White et al., 1992). A targeting vector was designed to replace the entire Cx50 coding region with a pgk-neo cassette. Transfection of ES cells with the targeting vector yielded two lines which were heterozygous at the Cx50 locus when analyzed by either PCR or Southern blotting of Nco1-digested genomic DNA (Fig. 1 b). The Southern analysis was limited to an internal probe, because suitable 5' or 3' flanking probes could not be obtained from the single Cx50 genomic clone isolated and used to construct the targeting vector. Efforts to isolate additional clones containing larger flanking regions were not successful. We are confident of the 5' genomic structure of the targeted locus because the PCR analysis used a 5' flanking primer, and the second Nco1 restriction site for Southern analysis is located in the 5' flanking DNA (White et al., 1992). However, without a 3' flanking probe, we cannot unequivocally verify the structure of the 3' end of the targeted locus. Injection of the Cx50-targeted clones into C57BL/6 blastocysts resulted in 18 male chimeric mice, four of which displayed germline transmission of the disrupted allele when bred with wild-type C57BL/6

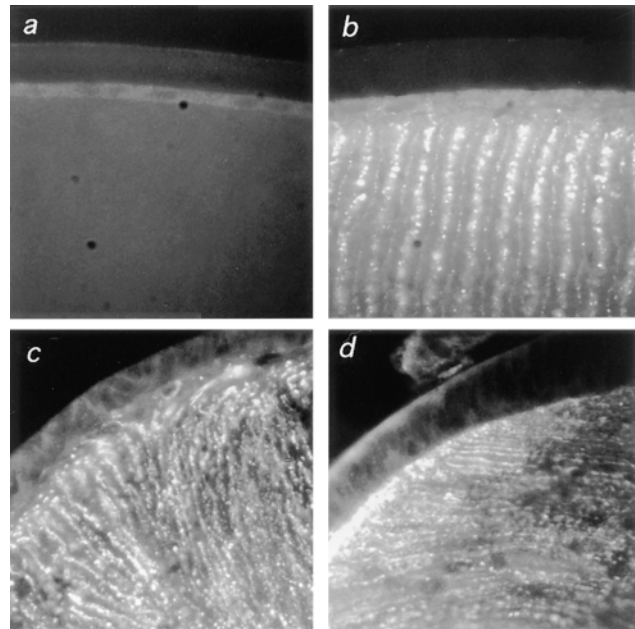


Figure 2. Immunohistochemical analysis of connexin expression in control and knockout lenses. (a) No signal was detected in knockout lenses with an anti-Cx50 antibody, whereas control littermates (b) showed a typical macular labeling of fiber cell membranes. (c) Cx46 continued to be expressed in the Cx50-knockout lenses with a fiber cell distribution similar to that seen in control lenses (d). Therefore, the loss of Cx50 did not grossly affect the distribution of Cx46 in lens fibers.

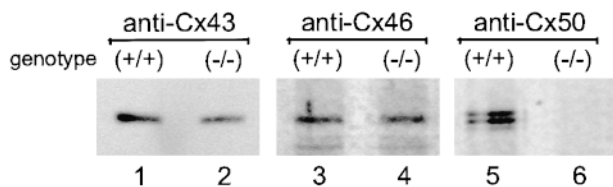


Figure 3. Cx43 and Cx46 expression levels in Cx50-knockout lens. Aliquots of membrane preparations of wild-type (lanes 1, 3, and 5) and knockout (lanes 2, 4, and 6) lenses containing equal protein concentrations were Western blotted with antibodies to Cx43 (lanes 1 and 2), Cx46 (lanes 3 and 4), and Cx50 (lanes 5 and 6). Both Cx43 and Cx46 continued to be expressed in knockout lenses at similar levels to those detected in the wild-type samples. As expected, Cx50 was not detected in the knockout lens.

females. Intercrossing of F1 heterozygous mice produced progeny of all three expected Cx50 genotypes (Fig. 1 *b*) in a 1:1.8:1 ratio ($n = 183$). Chimerae that displayed frequent germline transmission of the disrupted Cx50 allele were directly crossed with 129/Sv females to obtain knockout mice in the pure 129/Sv background. Equivalent phenotypes were observed in both mixed 129/Sv-C57BL/6 and pure 129/Sv genetic backgrounds. No phenotype was observed in Cx50 heterozygous animals in either genetic background.

Connexin Expression in Wild-type and Knockout Lenses

The deletion of Cx50 was confirmed by immunohistochemical analysis of control and knockout lenses. As expected, knockout mice no longer expressed Cx50 in their lens fibers (Fig. 2 *a*), whereas control littermates showed a typical macular labeling of fiber cell membranes (Kistler

et al., 1985) when stained with an anti-Cx50 antibody (Fig. 2 *b*). The distributions of Cx46 and Cx43 were also examined. Cx46 continued to be expressed in the Cx50-knockout lenses (Fig. 2 *c*), with a fiber cell distribution similar to that seen in control lenses (Fig. 2 *d*). Similarly, distribution of Cx43 in epithelial cells was comparable in knockout and control lenses (data not shown). Western blots of lenses probed with anti-Cx43 and anti-Cx46 antibodies revealed continued expression of these proteins in the knockout at levels compared with controls, whereas Cx50 was not detected in the knockout lens (Fig. 3). Thus, the loss of Cx50 did not grossly alter the quantity or distribution of the two remaining lens connexins.

Microphthalmia in Cx50-deficient Mice

Cx50-null mice were viable and fertile, and no differences were observed in the overall size of knockout and control animals. However, gross anatomical examination revealed that the eyes and lenses of Cx50-knockout mice were abnormally small in comparison to those from control littermates. To quantitate these differences, various organs were dissected from adult male control ($n = 17$) or Cx50-knockout ($n = 19$) mice and weighed (Fig. 4). No significant differences were observed in the average mass of the animals, or any of the weighed nonocular organs, as seen in the control data from kidney and testis shown in Fig. 4. In contrast, the masses of the eyes dissected from Cx50-knockout mice were 32% less ($P < 10^{-28}$, Student's unpaired *t* test), and the masses of the lenses were 46% less ($P < 10^{-24}$) when compared with control littermates. Thus, deletion of the Cx50 gene resulted in an ocular growth deficiency.

To determine when the growth deficit became apparent, the mass of animals, eyes, and lenses were recorded as a function of age. The overall postnatal growth was identical for Cx50-knockout and control mice (Fig. 5 *a*). Both eyes

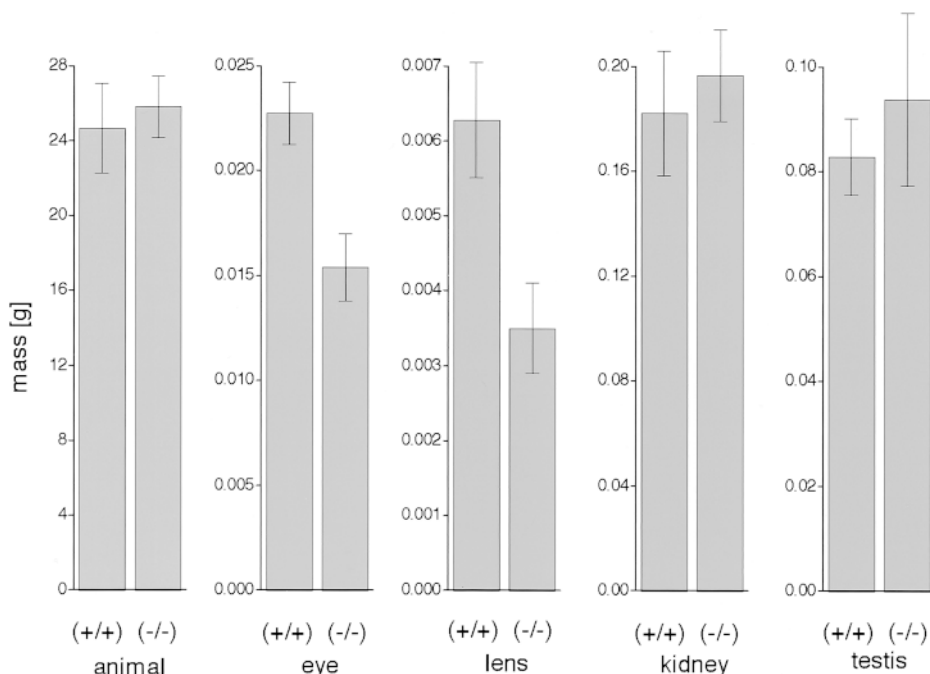


Figure 4. Cx50-knockout mice are microphthalmic. Gross anatomical examination revealed that the eyes and lenses of Cx50-knockout mice were abnormally small in comparison to those from control littermates. To quantitate these differences, eyes, lenses, and other control organs were dissected from adult male control ($n = 17$) or Cx50-knockout ($n = 19$) mice and weighed. No significant differences were observed in the average mass of the animals, their kidneys, or their testes. In contrast, the eyes dissected from Cx50-knockout mice were 32% smaller, and the lenses were 46% smaller when compared with control littermates. Thus, deletion of the Cx50 gene resulted in an ocular growth deficiency. Values are the mean \pm SD.

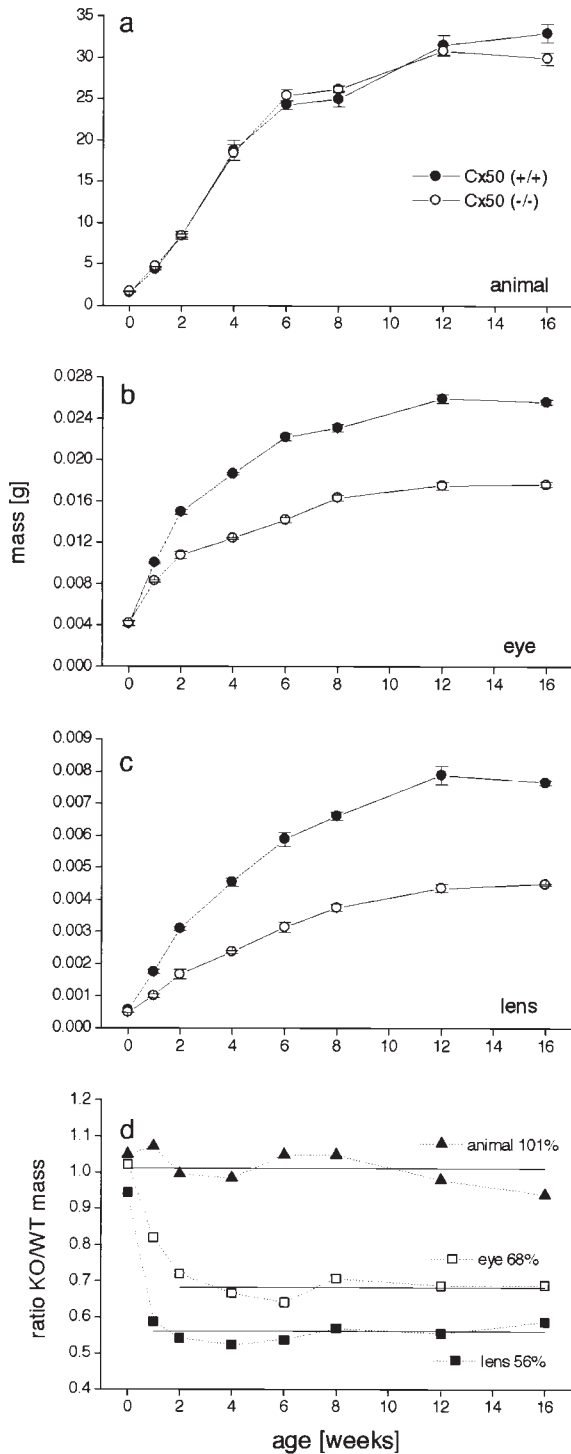


Figure 5. Lens and eye growth in Cx50-knockout mice. The mass of animals, eyes, and lenses were recorded as a function of age. (a) Overall postnatal growth was identical for Cx50-knockout and control mice. (b and c) Both eyes and lenses in the knockout animals grew over time, but the growth lagged that of control mice. (d) At P0, knockout eyes were identical to controls. At P7, knockout eyes weighed 82% as much as wild type, and by P14 the mass of knockout eyes was only 68% of control, a ratio which then remained constant throughout adulthood. Reduction of lens growth was even more striking. Again, masses were identical at P0, but by P7 the mass ratio was 56%, which remained constant thereafter. Thus, a transient inhibition of lens growth occurs in the first postnatal week in Cx50 knockouts. $n = 6-20$ at each time point. Values are the mean \pm SEM.

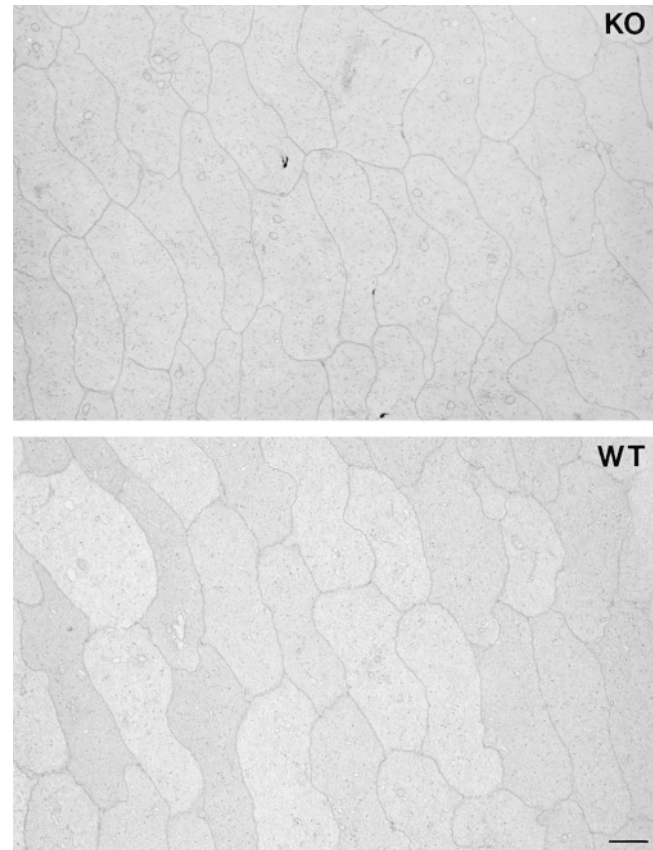


Figure 6. Electron microscopy of lens fibers. Coronal sections through the lens equator of Cx50^{-/-} (KO) and Cx50^{+/+} (WT) lenses revealed cross sections of synthetically active lens fibers with polyribosomes and mitochondria. Measurements of fiber diameter in these specimens revealed no significant differences between wild-type and knockout lenses. Bar, 1 μ m.

and lenses in the knockout animals grew over time, but the growth rate lagged that of control mice from an early age. At P0, eye mass in the Cx50-knockout mice was identical to controls but was decreased 18% by P7 (Fig. 5 b). By P14, the mass of a knockout eye was 68% that of control, a ratio which remained constant for at least 4 mo (Fig. 5, b and d). P0 lenses were too small to be accurately weighed, but their mass was estimated from their diameter (assuming a spherical shape and $\rho = 1$) which could be precisely measured. Masses were identical at P0, but by P7 the mass ratio was 56%, which remained constant thereafter (Fig. 5, c and d). These results suggest that embryonic ocular growth in Cx50-knockout mice is normal, but early postnatal growth is severely impaired.

The reduced mass of the lens could result from either fewer lens fibers due to a slowed rate of cell division or from the production of smaller lens fibers. Electron microscopic measurements of the diameters of lens fibers in the equatorial regions of wild-type and knockout lenses revealed no apparent differences in the sizes of the cells (Fig. 6), indicating that the cells were not systematically smaller in this dimension. Wild-type lens fibers had a diameter of $1.8 \pm 0.4 \mu\text{m}$ and knockout fibers had a diameter of $1.7 \pm 0.4 \mu\text{m}$ (mean \pm SD). These data suggested that the differ-

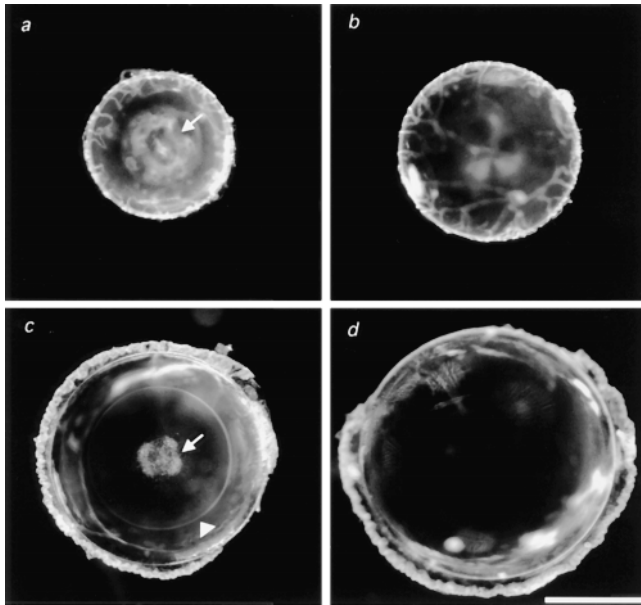


Figure 7. Nuclear cataracts in Cx50-knockout mice. (a) Lenses dissected from Cx50-knockout mice at P14 were smaller than those of control littermates (b) and exhibited an irregular and diffuse nuclear opacity (a, arrow) not present in control lenses. By 6 mo of age (c), knockout lenses had a fine particulate precipitate confined to the nucleus (c, arrow), characteristic of zonular pulverulent cataracts. In addition, a sharply defined line in the inner cortical region of the lens was present (arrowhead), the nature of which is not clear. (d) 6-mo-old control lenses had no light scattering opacities. Bar, 1 mm.

ence in size of knockout and wild-type lenses were due to fewer rather than smaller cells in the knockout lenses.

Cx50-knockout Mice Develop Cataracts

In mice, the eye opens and the lens begins to function at 2 wk of age (Kaufman, 1992). Lenses dissected from Cx50-knockout mice at this age were not only smaller than those of control littermates, but also exhibited an irregular and diffuse nuclear opacity (Fig. 7 a) not present in control lenses (Fig. 7 b). By 6 mo of age knockout lenses had a fine particulate precipitate confined to the nucleus, which is characteristic of zonular pulverulent cataracts (Fig. 7 c) (Nettleship, 1909). In addition, a sharply defined line in the inner cortical region of the lens was present. In contrast, 6-mo-old control lenses were much larger than knockout lenses, and had no light-scattering opacities (Fig. 7 d). Therefore, the absence of Cx50 resulted in perturbed lens homeostasis that induced cataract.

To examine early developmental stages of Cx50-knockout lenses for pathological changes, embryonic eyes and neonatal lenses were fixed, serially sectioned, and stained with hematoxylin and eosin. At E16.5, there were no differences in the size or integrity of lenses from either control (Fig. 8 a), or Cx50-knockout embryos (Fig. 8 b). At P7, control lenses had grown considerably, and the lens nuclei were stained with eosin (Fig. 8 c) in all of the serial sections. In contrast, knockout lenses were much smaller

and exhibited a clear zone in their nuclear region (Fig. 8 d). At higher magnification (Fig. 8 e), this clear zone was composed of fibers that had lost the strong eosinophilic staining seen in the cytoplasm of neighboring cells. Furthermore, fibers in the clear zone exhibited an irregularity of shape, reminiscent of swollen fibers (Kuwabara et al., 1969; Sakuragawa et al., 1975), although irregularities in shape have also been seen in normal adult human lenses (Taylor et al., 1996). These results showed that embryonic lens development was normal in knockout mice, but early postnatal growth was deficient and morphological changes were evident by P7.

Biochemical Analysis of Crystallins in Cx50-knockout Lenses

A characteristic feature of lens opacities is the conversion of soluble crystallins into an insoluble form (Piatigorsky, 1980), which was observed in the Cx46-knockout mice (Gong et al., 1997). In addition, those animals displayed an aberrant proteolytic cleavage of γ -crystallin which may have contributed to the loss of solubility. Therefore, the effect of the loss of Cx50 on the solubility and stability of crystallin proteins was examined. Control and knockout lenses from 6-mo-old animals were separated into soluble and insoluble components. Measured protein concentrations of these fractions were equivalent between wild-type and knockout in all cases except for the NaOH extraction, where the knockout lens had a twofold higher protein concentration in the supernatant. To permit comparison of Western blots, lanes of the gels of these fractions were loaded with equal volumes of each step of the extraction protocol and were then probed with antibodies to different crystallins. The final NaOH-insoluble pellet from both wild-type and knockout lenses was resuspended in one-tenth the volume of the other fractions. All of the crystallin proteins examined were abundant in the soluble fractions from either wild-type or knockout lenses. As expected, both α A- and α B-crystallins were detected in the insoluble fraction of Cx50-knockout lenses, but not wild-type lenses (Fig. 9, a and b). There were also clear differences in the solubility of γ -crystallin, and knockout lenses consistently showed a higher molecular weight aggregate of this protein (Fig. 9 c). In contrast to the Cx46-deficient mice, there were no low molecular weight polypeptides recognized by the γ -crystallin antibody in the Cx50-knockout lens. Silver-staining (Fig. 9 d) of the extracted lens fractions showed the highest concentrations of protein in the molecular weight range of the crystallins, as well as additional minor bands. One of these may have corresponded to the higher molecular aggregate recognized by the γ -crystallin antibody in the Western blot, none of the other bands was labeled by any of the anti-crystallin antibodies used.

Intercellular Communication in Cx50-deficient Lenses

To determine if the deletion of Cx50 perturbed normal patterns of gap junctional communication, we analyzed the intercellular passage of small dyes in control and knockout lenses. Embryonic lenses (E15.5) were dissected and either single lens fibers, or single epithelial cells, were impaled with microelectrodes containing Lucifer yellow

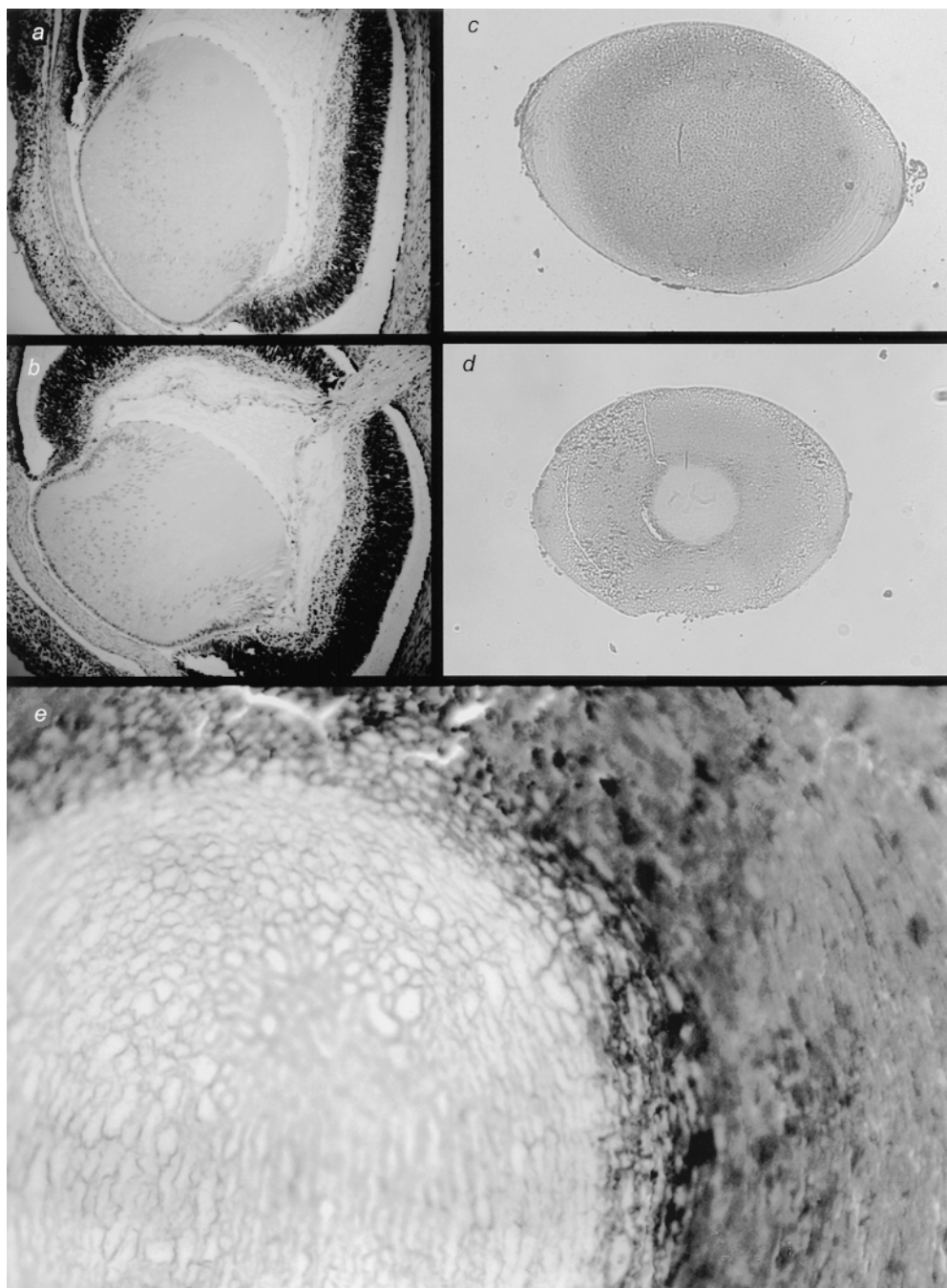


Figure 8. Growth deficiencies and pathological changes in Cx50-knockout lenses occur postnatally. Tissues were fixed, serially sectioned, and stained with hematoxylin and eosin. At E16.5, there were no differences in the size, or integrity of lenses from control (*a*) and Cx50-knockout (*b*) embryos. At P7, control lenses had grown considerably, and the lens nuclei were stained with eosin throughout the lens (*c*), whereas knockout lenses were much smaller and exhibited a large clear zone in their nuclear region (*d*). At higher magnification (*e*), this clear zone was composed of fiber cells lacking the normal eosinophilic staining.

and neurobiotin. Ionophoretic injection of Lucifer yellow into fiber cells resulted in an extensive dye spread, readily visible in whole lenses from either knockout (Fig. 10 *a*) or control (Fig. 10 *b*) animals. All injected lenses showed transfer of Lucifer yellow to neighboring cells (Cx50^{-/-}, *n* = 26; Cx50^{+/+}, *n* = 33), although there was variability in the extent of passage of the dye from injection to injection, independent of genotype. Transfer of neurobiotin, a much more sensitive probe of junctional communication, was also examined. After fiber injection, lenses were fixed, serially sectioned, and neurobiotin was visualized by incubation of sections with rhodamine-avidin. Extensive transfer of neurobiotin to many neighboring fiber cells was ob-

served in both the knockout (Fig. 10 *c*) and wild-type lenses (Fig. 10 *d*).

Also evident in both knockout and control lenses was an accumulation of neurobiotin in the overlying epithelium, which could result from either the leakage of tracer into epithelial cells during fiber penetration, or from fiber to epithelial cell junctional transfer, or contributions of both processes (Fig. 10, *c* and *d*). To distinguish between these two potential sources of epithelial cell staining, epithelial cells were directly impaled with dye-filled microelectrodes (Cx50^{-/-}, *n* = 4; Cx50^{+/+}, *n* = 5). These experiments were conducted such that only those lenses in which a stable resting potential was recorded throughout the experiment

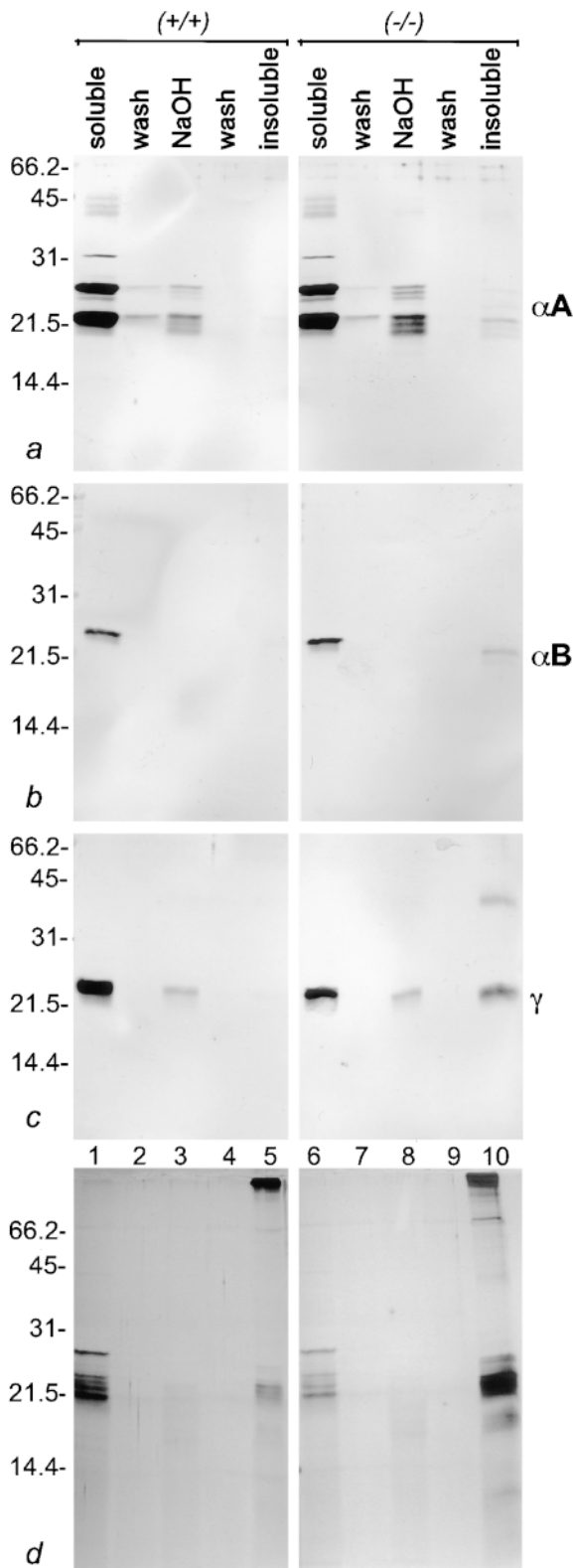


Figure 9. The effect of the loss of Cx50 on the solubility and stability of crystallin proteins. Wild-type (lanes 1–5) and knockout (lanes 6–10) lenses were homogenized and separated into soluble supernatants (lanes 1 and 6) and pellets by centrifugation. The pellets were then sequentially washed (lanes 2 and 7), extracted with NaOH (lanes 3 and 8), washed again (lanes 4 and 9), and the final insoluble pellets were resuspended (lanes 5 and 10). Equal volumes of all steps of the fractionation were Western blotted

were used. Monitoring of the lenses during injection revealed that the Lucifer yellow was injected only into the lens epithelium during the course of the experiment. These constraints insured that only a single lens epithelial cell received dye. Injection of single epithelial cells in knockout lenses resulted in transfer of Lucifer yellow to neighboring epithelial cells, but any transfer to the underlying fibers was below the threshold of detection (Fig. 10 *e*). In contrast, the neurobiotin dispersed widely through the epithelial cell layer and was easily detected in the underlying lens fibers (Fig. 10 *f*). Neurobiotin transfer to fibers was observed after all epithelial cell injections regardless of genotype ($n = 9$) except in one case, in which the epithelium had clearly separated from the underlying fibers during dissection. These results demonstrate that the targeted ablation of Cx50 did not eliminate gap junctional communication between epithelial cells, between fiber cells, or between the epithelium and the fibers in embryonic lenses up to developmental stage E15.5.

The presence of gap junctions between epithelial cells and lens fibers was also documented in the mouse lens by electron microscopy. Fig. 11 shows an electron micrograph of a gap junction joining the apical membrane of a lens epithelial cell with a lens fiber membrane (*arrowhead*). The terminal web, a marker of the apical epithelial cell cytoplasm (Jiang et al., 1995), is indicated (*TW*).

Discussion

Deletion of the Cx50 gene by homologous recombination resulted in reduced growth of the lens and eye, and the appearance of zonular pulverulent nuclear cataracts. Tracer injections indicated the persistence of intercellular communication between epithelial cells, between fiber cells, and between the epithelium and fibers up to developmental age E15.5 (Miller and Goodenough, 1986; Rae et al., 1996). Since we observed no alteration in the expression pattern of Cx46 and Cx43, we presume their continued presence accounted for this finding. In contrast to the Cx46-knockout (Gong et al., 1997), the deletion of Cx50 did not provoke detectable proteolysis of γ -crystallin proteins, although their conversion to insoluble forms contributed to cataractogenesis. These results demonstrate that Cx50-mediated intercellular communication is essential for multiple aspects of lens development and function. Comparison of these results with those obtained in the Cx46 knockout strongly suggests that the channel diversity

with anti-crystallin antibodies. α A-crystallin (*a*) and α B-crystallin (*b*) were detected in the insoluble fraction of Cx50-knockout lenses, but not wild-type lenses. (*c*) Differences in the solubility of γ -crystallin were also detected and knockout lenses consistently showed a higher molecular weight aggregate of this protein. In contrast to the Cx46 knockout, no lower molecular weight proteolytic fragments of γ -crystallin were detected with the γ -crystallin antibody in the Cx50-knockout lens. (*d*) Silver-stained gel of the extracted lens fractions. The majority of insoluble proteins in the knockout lens were in the molecular weight range of the crystallins, although additional minor bands were also present.

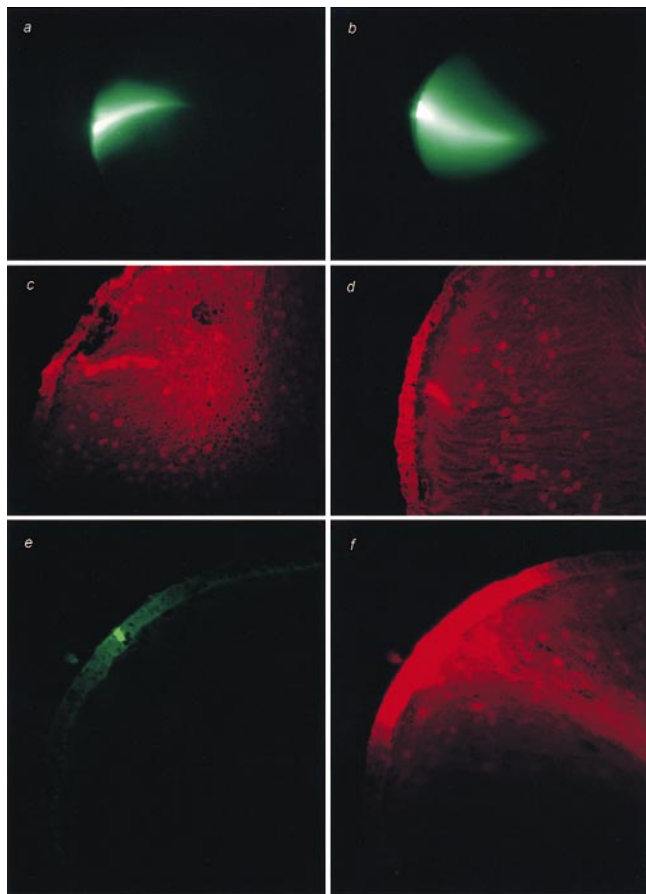


Figure 10. Targeted ablation of Cx50 did not eliminate gap junctional communication between epithelial cells, between fiber cells, or between the epithelium and the fibers. Intercellular communication in E15.5 embryonic lenses was assessed by intracellular injection of low molecular mass tracers. Single lens fibers were impaled with microelectrodes containing Lucifer yellow and neurobiotin. During the injections into whole lenses, the spread of Lucifer yellow (*green*) between fibers was readily detected in both knockout (*a*) and control (*b*) lenses. After injection, lenses were fixed and paraffin sections were stained with rhodamine-avidin to label neurobiotin (*red*). Extensive transfer of neurobiotin to many neighboring fiber cells was observed in both the knockout (*c*) and control (*d*) lenses. Epithelial to fiber communication was tested by microinjection of single epithelial cells with Lucifer yellow and neurobiotin. (*e*) Injection of a single epithelial cell in a knockout lens resulted in a weak transfer of Lucifer yellow to neighboring epithelial cells, but transfer to the underlying fibers was below the threshold of detection. In contrast, the neurobiotin dispersed widely through the epithelial cell layer and was easily detected in the underlying lens fibers (*f*).

resulting from the expression of two connexins in lens fibers is required.

Dye injection studies revealed that the pathways of lens intercellular communication were not detectably altered as a result of the loss of Cx50. Both Lucifer yellow and neurobiotin injected into single lens fibers diffused to adjacent fibers throughout the lens. There has been controversy surrounding the presence of a gap junctional communication pathway between epithelial cells and lens fibers (Basnet et al., 1994). We observed that Lucifer yellow

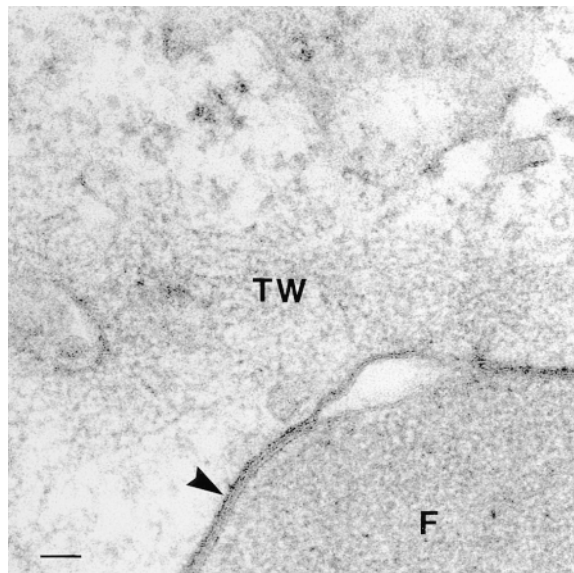


Figure 11. Electron microscopy of the epithelium/fiber interface in a Cx50^{+/+} lens. Occasional heptalaminar gap junctions (*arrowhead*) were found joining epithelial cells and lens fibers. Epithelial cell apical surfaces were characterized by a terminal web of actin filaments (*TW*) and the fiber (*F*) by its dense protein-rich cytoplasm and lack of cellular organelles. Bar, 60 nm.

injected into individual epithelial cells diffused within the plane of the epithelium, but could not be detected in the underlying fibers. It is clear from earlier studies (Miller and Goodenough, 1986; Rae et al., 1996) that the rate of transfer of Lucifer yellow between epithelium and fiber is slow and difficult to detect. However, we observed substantive epithelium to fiber transfer of the more sensitive probe neurobiotin, in addition to documenting the morphological presence of gap junctions at this cell-cell interface. Importantly, regardless of how epithelial cells and fibers are joined into a functional syncytium, we observed no differences in the communication patterns between wild-type and knockout lenses at developmental stages before cataract formation. We would expect that after the morphological expression of cataract and the concomitant death of lens fibers, that there will be substantive changes in gap junctional communication pathways between the affected cells.

The microphthalmia exhibited in the Cx50-knockout animals is likely to result in part from the retardation of lens growth. Studies of chick eye embryogenesis after extirpation of the lens indicate that normal lens development is required for the growth of the eye (Coulombre and Coulombre, 1964). Furthermore, ablation of the growing lens by transgenic expression of toxic genes had a similar effect on eye growth in mice (Breitman et al., 1987; Landel et al., 1988). Although the rate of eye growth slowed in parallel with the rate of lens growth immediately after birth, the eye growth rate continued to decrease for 1 wk after the lens growth rate had stabilized. Thus, other influences, in addition to factors from the lens, may be contributing to the size of the eye during this postnatal period. In turn, the reduction in lens size appears to result from a transient in-

hibition of growth rate during the first postnatal week. Growth rates before and after this critical period are not significantly different than controls. The retardation in growth affects only the formation of secondary lens fibers, a process that continues throughout life, but is much more active in the early postnatal period. Measurement of lens fiber diameter indicated that the reduction of lens size was the result of fewer lens fibers.

Cx50 knockouts display a transient reduction in eye and lens growth during early postnatal development, indicating that intercellular communication subserves multiple functions. Cataractogenesis, seen with both connexin knockouts, indicates that Cx46 and Cx50 have a shared function in the circulation and flow of ions, metabolites, and water through the lens. Cx50, in contrast to Cx46, must have an additional, novel function, the absence of which results in the temporally discrete slowing of the rate of cell proliferation. This does not appear to be a growth arrest but a coordinated increase in the duration of the cell cycle in a population of mitotically active cells. The acute and transient decrease in rate reveals both a specific requirement for Cx50 and a critical time in lens growth, the period between P0 and P7.

One explanation for the restriction of the growth phenotype to loss of Cx50 but not Cx46 is that an early postnatal growth signal can propagate efficiently through Cx50 but not Cx46 channels. Alternatively, at the critical time in development, there could be differences in the spatial/temporal patterns of expression for Cx50 and Cx46, which are beyond the detection limit of light microscopy. If Cx50 expression precedes that of Cx46 during fiber development, then differentiation could be transiently delayed until the appearance of Cx46 and the restoration of appropriate communication. In the avian lens, there are no gross differences in spatial or temporal expression patterns of the orthologs of Cx50 and Cx46, which are expressed in both the lens epithelium and fibers (Jiang et al., 1995). However, only Cx50 expression has been studied during lens differentiation in rodents (Evans et al., 1993), and it has not been determined if Cx50 is present in epithelial cells.

The growth defect in Cx50 knockouts suggests that Cx50 is present in the mitotically active epithelial cells. In sections of intact lens, it is difficult to detect Cx50 in epithelial cells due to the intense staining in the underlying fibers. This problem can be partially overcome by separation of the epithelium from the fiber mass by manual removal of the lens capsule, to which the epithelial cells adhere (Jiang et al., 1995). Antibodies specific for Cx50 positively stained epithelial cells in these preparations (data not shown). Thus, it is likely that Cx50 is expressed in rodent epithelium, similar to chicken lens epithelial cells (Jiang et al., 1995) although we cannot rule out the possibility of fiber contamination. Ultimate resolution of this question will require ultrastructural analysis of the rodent lens epithelium.

Together, the Cx46 and Cx50 knockout studies strongly suggest that the presence of intercellular channels with different functional properties is necessary for normal lens homeostasis. However, our data do not directly address the effect of changes in levels of communication. Due to variability in dye transfer between lens cells in both wild-type and knockout lenses, our physiological data do not

permit a quantitative comparison of communication levels. Given no substantive upregulation of Cx46 in the Cx50-knockout animals, it is possible that decreased absolute levels of intercellular channels account for some of the observed phenotypic changes.

Cx50-knockout mice develop a zonular pulverulent cataract at an early postnatal age. A human congenital zonular pulverulent cataract (CZP1, OMIM 116200) in a six-generation English kindred (Renwick and Lawler, 1963) has recently been mapped to the vicinity of the human Cx50 gene. Sequence analysis of the coding region of Cx50 in affected members of this pedigree detected a C→T transition in codon 88 resulting in the nonconservative substitution of serine for proline (Shiels et al., 1998). Although the effect of this mutation on the activity of Cx50 has not been directly tested, it is likely to result in a functional change in channel activity, as the same mutation in human Cx32 underlies a form of peripheral neuropathy, CMTX1 (Janssen et al., 1997). Therefore, the Cx50-knockout mice provide a model to study the early cellular events leading to the cataractous changes associated with this human disease.

We thank J. Horwitz for the generous gift of anti-crystallin antibodies, E. Li for blastocyst injections, and D. Beebe (Washington University, St. Louis, MO) and X. Gong (Scripps Institute, La Jolla, CA) for helpful discussion. We also thank B. Keon and C. Sellitto (both from Harvard Medical School, Boston, MA) for comments on the manuscript.

This work was supported by grants from the National Institutes of Health to D.L. Paul (GM-37751) and D.A. Goodenough (EY-02430).

Received for publication 27 April 1998 and in revised form 10 September 1998.

References

- Basnet, S., J.R. Kuszak, L. Reinisch, H.G. Brown, and D.C. Beebe. 1994. Intercellular communication between epithelial and fiber cells of the eye lens. *J. Cell Sci.* 107:799–811.
- Beyer, E.C., J. Kistler, D.L. Paul, and D.A. Goodenough. 1989. Antisera directed against connexin43 peptides react with a 43-kD protein localized to gap junctions in myocardium and other tissues. *J. Cell Biol.* 108:595–605.
- Blum, H., H. Beier, and M. Gross. 1987. Improved silver staining of plant proteins, RNA and DNA in polyacrylamide gels. *Electrophoresis.* 8:93–99.
- Breitman, M.L., S. Clapoff, J. Rossant, L.-C. Tsui, L.M. Glode, I.H. Maxwell, and A. Berstein. 1987. Genetic ablation: targeted expression of a toxin gene causes microphthalmia in transgenic mice. *Science.* 238:1563–1565.
- Bruzzone, R., T.W. White, and D.L. Paul. 1996. Connections with connexins—the molecular basis of direct intercellular signaling [Review]. *Eur. J. Biochem.* 238:1–27.
- Coulombre, A.J., and J.L. Coulombre. 1964. Lens development 1. Role of the lens in eye growth. *J. Exp. Zool.* 156:39–48.
- Evans, C.W., S. Eastwood, J. Rains, W.T.M. Gruijters, S. Bullivant, and J. Kistler. 1993. Gap junction formation during development of the mouse lens. *Eur. J. Cell Biol.* 60:243–249.
- Goliger, J.A., and D.L. Paul. 1994. Expression of gap junction proteins Cx26, Cx31.1, Cx37, and Cx43 in developing and mature rat epidermis. *Dev. Dynam.* 200:1–13.
- Gong, X., E. Li, G. Klier, Q. Huang, Y. Wu, H. Lei, N. Kumar, J. Horwitz, and N.B. Gilula. 1997. Disruption of α_3 connexin gene leads to proteolysis and cataractogenesis in mice. *Cell.* 91:933–943.
- Goodenough, D.A. 1979. Lens gap junctions: a structural hypothesis for non-regulated low-resistance intercellular pathways. *Invest. Ophthalmol. Vis. Sci.* 18:1104–1122.
- Goodenough, D.A., J.S.B. Dick II, and J.E. Lyons. 1980. Lens metabolic cooperation: a study of mouse lens transport and permeability visualized with freeze-substitution autoradiography and electron microscopy. *J. Cell Biol.* 86:576–589.
- Janssen, E.A.M., S. Kemp, G.W. Hensels, O.G. Sie, C.E.M. Dediesmulders, J.E. Hoogendijk, M. Devisser, and P.A. Bolhuis. 1997. Connexin32 gene mutations in x-linked dominant charcot-marie-tooth disease (cmtx1). *Hum. Genet.* 99:501–505.
- Jiang, J.X., T.W. White, and D.A. Goodenough. 1995. Changes in connexin expression and distribution during chick lens development. *Dev. Biol.* 168: 649–661.

- Kaufman, M.H. 1992. *The Atlas of Mouse Development*. Academic Press, London, UK. 508 pp.
- Kistler, J., B. Kirkland, and S. Bullivant. 1985. Identification of a 70,000-D protein in lens membrane junctional domains. *J. Cell Biol.* 101:28–35.
- Kumar, N., and N.B. Gilula. 1996. The gap junction communication channel. *Cell.* 84:381–388.
- Kuwabara, T., J.H. Kinoshita, and D.G. Cogan. 1969. Electron microscopic study of galactose induced cataract. *Invest. Ophthalmol. Vis. Sci.* 8:133–145.
- Landel, C.P., J. Zhao, D. Bok, and G.A. Evans. 1988. Lens-specific expression of recombinant ricin induces developmental defects in the eyes of transgenic mice. *Genes Dev.* 2:1168–1178.
- Li, E., T.H. Bestor, and R. Jaenisch. 1992. Targeted mutation of the DNA methyltransferase gene results in embryonic lethality. *Cell.* 69:915–926.
- Mathias, R.T., J.L. Rae, and G.J. Baldo. 1997. Physiological properties of the normal lens. *Physiol. Rev.* 77:21–50.
- Miller, T.M., and D.A. Goodenough. 1986. Evidence for two physiologically distinct gap junctions expressed by the chick lens epithelial cell. *J. Cell Biol.* 102:194–199.
- Nettleship, E. 1909. Seven new pedigrees of hereditary cataract. *Trans. Ophthalmol. Soc. UK.* 29:188–211.
- Paul, D.L., L. Ebihara, L.J. Takemoto, K.I. Swenson, and D.A. Goodenough. 1991. Connexin46, a novel lens gap junction protein, induces voltage-gated currents in nonjunctional plasma membrane of *Xenopus* oocytes. *J. Cell Biol.* 115:1077–1089.
- Piatigorsky, J. 1980. Intracellular ions, protein metabolism, and cataract formation. *Curr. Top. Eye Res.* 3:1–39.
- Piatigorsky, J. 1981. Lens differentiation in vertebrates. A review of cellular and molecular features. *Differentiation.* 19:134–153.
- Rae, J.L. 1979. The electrophysiology of the crystalline lens. *Curr. Top. Eye Res.* 1:37–90.
- Rae, J.L., C. Bartling, J. Rae, and R.T. Mathias. 1996. Dye transfer between cells of the lens. *J. Membr. Biol.* 150:89–103.
- Renwick, J.H., and S.D. Lawler. 1963. Probable linkage between a congenital cataract locus and the Duffy blood group locus. *Ann. Hum. Genet.* 27:67–84.
- Sakuragawa, M., T. Kuwabara, J.H. Kinoshita, and H.N. Fukui. 1975. Swelling of the lens fibers. *Exp. Eye Res.* 21:381–394.
- Shiels, A., D. Mackay, A. Ionides, V. Berry, A. Moore, and S. Bhattacharya. 1998. A missense mutation in the human connexin50 gene (*gja8*) underlies autosomal dominant zonal pulverulent cataract, on chromosome 1q. *Am. J. Hum. Genet.* 62:526–532.
- Taylor, V.L., K.J. Al-Ghoul, C.W. Lane, V.A. Davis, J.R. Kuszak, and M.J. Costello. 1996. Morphology of the normal human lens. *Invest. Ophthalmol. Vis. Sci.* 37:1396–1410.
- White, T.W., R. Bruzzone, D.A. Goodenough, and D.L. Paul. 1992. Mouse Cx50, a functional member of the connexin family of gap junction proteins, is the lens fiber protein MP70. *Mol. Biol. Cell.* 3:711–720.
- White, T.W., R. Bruzzone, S. Wolfram, D.L. Paul, and D.A. Goodenough. 1994. Selective interactions among the multiple connexin proteins expressed in the vertebrate lens: the second extracellular domain is a determinant of compatibility between connexins. *J. Cell Biol.* 125:879–892.